

ARTICLE

Thickness Impacts of Vacancy Defects in Epitaxial $\text{La}_{0.7}\text{Sr}_{0.3}\text{MnO}_3$ Thin Films Using Slow Positron Beam

Jian-dang Liu, Bin Cheng, Huai-jiang Du, Bang-jiao Ye*

Department of Modern Physics, University of Science and Technology of China, Hefei 230026, China

(Dated: Received on June 8, 2010; Accepted on October 8, 2010)

Thickness effects of thin $\text{La}_{0.7}\text{Sr}_{0.3}\text{MnO}_3$ (LSMO) films on $(\text{LaAlO}_3)_{0.3}(\text{Sr}_2\text{AlTaO}_6)_{0.7}$ (LAST (001)) substrates were examined by a slow positron beam technique. Doppler-broadening line shape parameter S was measured as a function of thickness and different annealing conditions. Results reveal there could be more than one mechanism to induce vacancy-like defects. It was found that strain-induced defects mainly influence the S value of the *in situ* oxygen-ambient annealing LSMO thin films and the strain could vanish still faster along with the increase of thickness, and the oxygen-deficient-induced defects mainly affect the S value of post-annealing LSMO films.

Key words: Thin film, Giant magnetoresistance, Slow positron beam, Defect

I. INTRODUCTION

Since the observation of giant magnetoresistance (GMR) effect in perovskitelike films [1, 2], the hole-doped manganese oxides $\text{La}_{1-x}\text{A}_x\text{MnO}_3$ (where A=divalent alkaline-earth ions, such as Ca, Sr, and Ba) have been extensively studied in the latest few decades [1–4]. GMR films have many novel physical properties, such as metal-insulator transition, new electron, and spin transport properties [1–7]. Recently, new research shows that the ferromagnetic transition T_c , resistivity ρ , and magnetoresistance of strained GMR thin films are all related to the grain boundaries, the magnetic domain boundaries, and the film stress [8–11]. What's more, recent study also revealed that the capability of the capacitors would be affected by oxygen vacancies and related defect-dipole complexes [5, 6]. It is important to investigate the defect morphology and microstructure in GMR thin-film research.

Positrons have been widely used to study the crystal structure and it is well known that they preferentially trap into open-volume defects such as vacancies [12]. Doppler-broadening spectroscopy is used to characterize defect structures, and the nature is an electron momentum spectroscopy which employ high-resolution energy detector to obtain the annihilation line-shape. Slow positron beam technique is employed to obtain the defect depth profile, which can adjust the positron energy in a range of a few eV to several tens of keV [12–15], and the monoenergetic positrons are obtained by moderation. Once the positron is extracted from the

moderator, it is magnetically guided through a vacancy system and then implanted into condensed matter. To analyze the obtained Doppler-broadening energy spectrum, the line-shape parameter S is introduced which is defined as the ratio of the area of a suitably selected central region of the energy spectrum versus the entire area [16]. In order to get maximum information out of the parameters, a proper choice of the energy windows is important. The central window for S is chosen so that it covers about 50% of the total peak. Once the measurement of slow positron beam experiment finished, the S - E curves can be obtained and also gained the depth profile of defects distribution.

In this work, we investigated the thickness effects in epitaxial $\text{La}_{0.7}\text{Sr}_{0.3}\text{MnO}_3$ (LSMO) thin films on $(\text{LaAlO}_3)_{0.3}(\text{Sr}_2\text{AlTaO}_6)_{0.7}$ (LAST) by slow positron beam technique. Two series samples were studied. The distinct change of S parameter and positron's effective diffusion length L_{eff} as the function of films thickness were also studied. The vacancy defects due to the strain relax and the oxygen-deficient annealing were analyzed, which can trap positrons and cause S and positron effective diffusion length L_{eff} change sensitively.

II. EXPERIMENTS

Epitaxial LSMO thin films were deposited on LAST substrates using the pulsed laser deposition method. An excimer KrF laser ($\lambda=248$ nm) was used to ablate sintered polycrystalline LSMO target. The deposition laser repetition rate was 10 Hz. The deposition chamber was evacuated to a base pressure of 50 μPa before deposition. The samples deposited temperature was 750 $^\circ\text{C}$, whereas the deposition oxygen pressure was 26 Pa. Different thickness samples, which are about 7.5, 11, 35,

* Author to whom correspondence should be addressed. E-mail: bjye@ustc.edu.cn

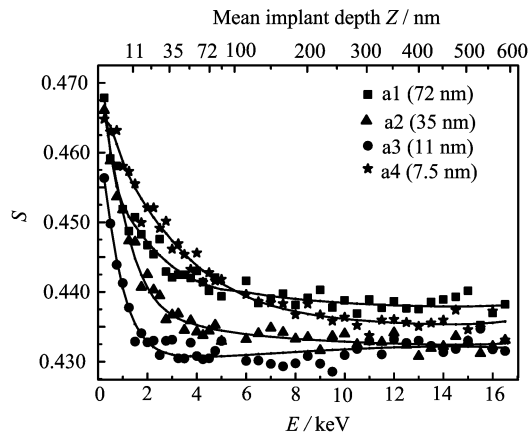


FIG. 1 S parameter as a function of the incident positron energy E for the LSMO/LAST samples annealing in air. The solid curves are fitted results by VEPFIT.

and 72 nm respectively, were deposited. Thereafter, one series of four samples (named a1, a2, a3, and a4 respectively) were annealed at 750 °C in air for 2 h before being cooled to room temperature, the other series of four samples (named b1, b2, b3, and b4 respectively) were annealed at 750 °C in 26 Pa oxygen ambience for 2 h and *in situ* cooled to room temperature.

The defect depth profile was carried out using a variable energy positron beam technique which can change energy from 0.25 keV to 16.5 keV. A high purity Ge detector with a resolution of 1.2 keV at 514 keV γ -rays of ^{85}Sr was used to measure the Doppler broadening spectrum. The total net counts of each spectrum were about 2×10^5 . The S parameter was used to analyze the Doppler broadening spectrum. The S parameter in this measurement is defined as the ratio of the central region (511 ± 1 keV) to the total area of 511 keV annihilation peak. The S - E curves were fitted using VEPFIT program [17].

III. RESULTS AND DISCUSSION

Figures 1 and 2 show the S parameter of LSMO/LAST versus the incident positron energy E . The solid curves are the fitting results. The shape of all S - E curves is consistent with positron annihilation in typical LSMO films [18]. The positron mean implantation depth Z is also shown at top horizontal axis.

It is easy to observe that all S - E curves monotonically fall. When the implantation energy is low, positrons were mainly trapped by surface defects or formed positroniums (a bound state between a positron and an electron) which enlarged S value. As the positron implantation energy increases, more positrons annihilated in LSMO thin films and fewer positrons diffused back to the surface and annihilated at the surface. And the S value displays a common feature. But when the incident positron energy increased even higher, a

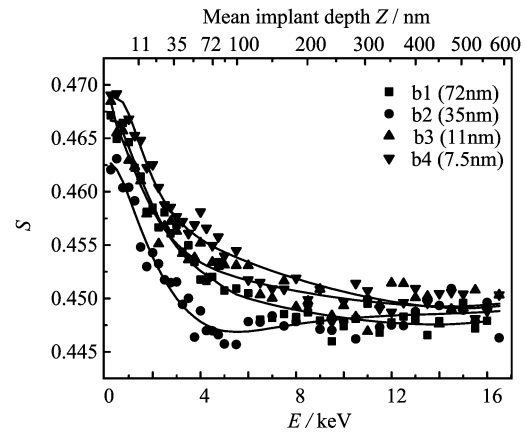


FIG. 2 S parameter as a function of the incident positron energy E for the LSMO/LAST samples annealing in oxygen ambience. The solid curves are fitted results by VEPFIT.

TABLE I Fitting results of samples a1, a2, a3, and a4 which were annealed in air for 2 h.

Sample	Thickness/nm	S_{LSMO}	L_{eff}/nm
a1	7.5	0.4545 ± 0.0008	1.8 ± 0.4
a2	11	0.4355 ± 0.0009	17.9 ± 0.6
a3	35	0.4370 ± 0.0009	16.2 ± 0.8
a4	72	0.4418 ± 0.0004	2.9 ± 0.8

TABLE II Fitting results of samples b1, b2, b3, and b4 which were annealed in oxygen ambience for 2 h.

Sample	Thickness/nm	S_{LSMO}	L_{eff}/nm
b1	7.5	0.4541 ± 0.0004	14.0 ± 1.4
b2	11	0.4515 ± 0.0003	18.0 ± 1.2
b3	35	0.4446 ± 0.0004	22.4 ± 1.8
b4	72	0.4496 ± 0.0009	21.5 ± 1.7

plateau region appeared, which indicates that positrons were mainly annihilated in LAST substrates.

The VEPFIT program was used to fit the measured results. Table I and Table II show the fitting S value and L_{eff} . S is fitted as:

$$S = S_s f_s + S_{\text{LSMO}} f_{\text{LSMO}} + S_{\text{LAST}} f_{\text{LAST}} \quad (1)$$

where S_s , S_{LSMO} , and S_{LAST} are the S parameters for the positrons annihilated at the surface, in LSMO film, and in substrate respectively, and f_s , f_{LSMO} , and f_{LAST} are the fractions of positrons annihilated at the surface, in LSMO film, and in substrate respectively.

As can be seen from Table I and Table II, the S value of the *in situ* annealing samples is non-monotonic changes as the function of films thickness decreases, but the monotonic change tendency for all oxygen-ambience annealing samples is observed. Thereafter, it is recognized that there could be more than one mechanism to induce vacancy-like defects.

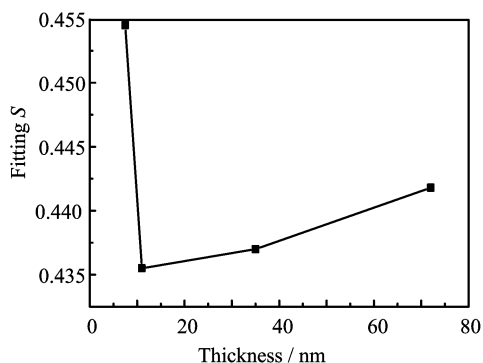


FIG. 3 S value versus the thickness of samples a1, a2, a3, and a4.

Epitaxial LSMO films deposited on the substrates have the lattice mismatch,

$$m = \frac{a - a_{\text{sub}}}{a_{\text{sub}}} \quad (2)$$

where a and a_{sub} are the lattice constant of LSMO and substrate respectively [19]. In this experiment, $a=3.873 \text{ \AA}$, $a_{\text{sub}}=3.868 \text{ \AA}$, so all films are under pressure stress with $m=0.13\%$. Valencia *et al.* studied the strain-induced charge depletion in $\text{La}_{2/3}\text{Ca}_{1/3}\text{MnO}_3$ epitaxial thin films and implied that introduction of oxygen vacancies in the as-grown films could minimize elastic energy in strained films [20]. Besides, as the result of strain, these vacancies cannot disappear even annealing in oxygen ambience.

In order to realize the impact of vacancy defects with the thickness clearly, the thickness dependence of S is plotted in Fig.3 and Fig.4. In Fig.3, the S value increases along with the films thickness increases of samples a2, a3, and a4, indicating that the defects concentration increases along with the films growth. Previously, Jin *et al.* reported that even deposited epitaxial $\text{Nd}_{0.7}\text{Sr}_{0.3}\text{MnO}_3$ (NSMO) thin films at an oxygen pressure of 35 Pa also have more oxygen-deficient and strain-effect related to oxygen vacancies [21]. It should be noted that the lattice structure of the LSMO films is similar to that of the NSMO. But here, the LSMO films is deposited at a lower oxygen pressure of 26 Pa. Therefore, we conclude that our two series samples were all deposited in an oxygen-deficient ambience, and lots of oxygen vacancies in LSMO films were induced. The large S value and short L_{eff} for LSMO films can be ascribed to oxygen-vacancies trap positrons.

Moreover, as films grow in the same chamber ambience, the thicker the films growth, the more oxygen needed, and it could induce more oxygen-deficient defects. Consequently, the S value increases along with the films thickness increases of samples a2, a3, and a4. But sample a1 has an opposite tendency. Its reason could be that the thinner film (such as a1, thickness of 7.5 nm only) has not enough thickness to relax its pressure stress and have more mismatch defects comparing

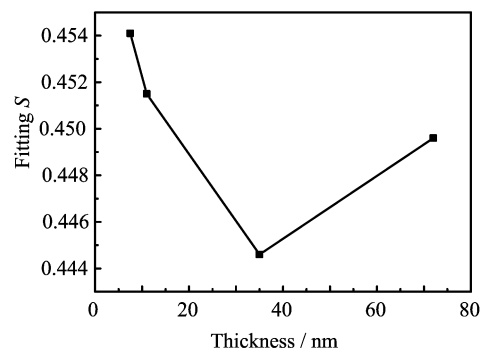


FIG. 4 S value versus the thickness of samples b1, b2, b3, and b4.

with the defects caused by oxygen-deficient.

Figure 4 shows the S value monotonic decrease versus the thickness increase of samples b1, b2, and b3, from $S_{\text{LSMO}}=0.4541$ to 0.4446. But the S value of sample b4 appears abnormal. Even though all the four samples were annealed for 2 h in oxygen ambience, the oxygen vacancies were not all filled in with the diffusion oxygen atoms of sample b4 due to the thickness and oxygen-deficient caused vacancies also exist and trap positrons. For the thinner films b1, b2, and b3, the main oxygen-deficient induced defects could be vanishing, and positron was mainly trapped by the strain caused defects. In other words, the monotonic change of S value reflects the relax degree of strain. Therefore, we could conclude that along with the films thickness increases, the defects induced by lattice mismatch become much less and the pressure stress release much faster. Razavi *et al.* also has the similar result [9].

IV. CONCLUSION

Epitaxial LSMO thin films were deposited on LAST substrates using the pulsed laser deposition method. A slow positron beam technique was employed to probe the vacancy defects of the films under different condition. The line shape parameter S of two series samples was measured as a function of the incident positron energy E . The results indicate that it could be more than one mechanism to induce vacancy-like defects. We have found that strain-induced defects mainly influence the S value of the *in situ* oxygen-ambience annealing LSMO thin films and the strain could vanish still faster as the thickness increase, and the oxygen-deficient-induced defects mainly influence the S value of post-annealing LSMO films.

V. ACKNOWLEDGMENTS

This work was supported by the National Natural Science Foundation of China (No.10835006). Jian-dang Liu is grateful to Ph.D Cheng-xiao Peng, Shao-wei Jin,

and Xiang-lei Chen for enlightening discussions and other colleagues' enjoyable collaboration.

- [1] M. Imada, A. Fujimori, and Y. Tokura, *Rev. Mod. Phys.* **70**, 1039 (1998).
- [2] R. Von Helmolt, J. Wecker, B. Holzapfel, L. Schultz, and K. Samwer, *Phys. Rev. Lett.* **71**, 2331 (1993).
- [3] Y. H. Xiong, X. C. Bao, J. Zhang, C. L. Sun, W. H. Huang, X. S. Li, Q. J. Ji, X. W. Cheng, Z. H. Peng, N. Lin, Y. Zeng, Y. F. Cui, and C. S. Xiong, *Phys. B* **398**, 102 (2007).
- [4] J. Zhang, H. Tanaka, T. Kanki, J. H. Choi, and T. Kawai, *Phys. Rev. B* **64**, 184404 (2001).
- [5] W. B. Wu, K. H. Wong, C. L. Choy, and Y. H. Zhang, *Appl. Phys. Lett.* **77**, 3441 (2000).
- [6] W. B. Wu, K. H. Wong, C. L. Choy, and Y. H. Zhang, *Thin Solid Films* **389**, 56 (2001).
- [7] E. Dagotto, *Science* **309**, 257 (2005).
- [8] M. Ziese, *Rep. Prog. Phys.* **65**, 143 (2002).
- [9] F. S. Razavi, G. Gross, H. U. Habermerier, O. Lebedev, S. Amelinckx, G. Van Tendeloo, and A. Vigliante, *Appl. Phys. Lett.* **76**, 155 (2000).
- [10] X. J. Chen, S. Soltan, H. Zhang, and H. U. Habermerier, *Phys. Rev. B* **65**, 174402 (2002).
- [11] P. Murugavel, J. H. Lee, J. G. Yoon, T. W. Noh, J. S. Chung, M. Heu, and S. Yoon, *Appl. Phys. Lett.* **82**, 1908 (2003).
- [12] P. J. Schulz and K. G. Lynn, *Rev. Mod. Phys.* **60**, 701 (1988).
- [13] H. Weng, D. Wang, R. Han, Y. Jiang, G. Yang, and X. Liu, *Mater. Sci. Engin. B* **26**, 163 (1994).
- [14] H. M. Weng, X. Y. Zhou, B. J. Ye, J. F. Du, and R. D. Han, *Physics* **29**, 308 (2000).
- [15] C. X. Peng, H. M. Weng, X. J. Yang, B. J. Ye, B. Cheng, X. Y. Zhou, and R. D. Han, *Chin. Phys. Lett.* **23**, 489 (2006).
- [16] I. K. MacKenzie, J. A. Eady, and R. R. Gingerich, *Phys. Lett. A* **33**, 279 (1970).
- [17] A. van Veen, H. Schut, M. Clement, J. M. M. de Nijs, A. Kruseman, and M. R. Ijpma, *Appl. Surf. Sci.* **85**, 216 (1995).
- [18] S. W. Jin, X. Y. Zhou, W. B. Wu, C. F. Zhu, H. M. Weng, H. Y. Wang, X. F. Zhang, B. J. Ye, and R. D. Han, *J. Phys. D* **37**, 1841 (2004).
- [19] C. Aruta, G. Ghiringhelli, A. Tebano, N. G. Boggio, N. B. Brookes, P. G. Medaglia, and G. Balestrino, *Phys. Rev. B* **73**, 235121 (2006).
- [20] S. Valencia, L. Balcells, J. Fontcuberta, and B. Martinez, *Appl. Phys. Lett.* **82**, 4531 (2003).
- [21] S. W. Jin, W. B. Wu, H. M. Weng, B. J. Ye, and X. Y. Zhou, *J. Phys. D* **39**, 4125 (2006).